TELKOMNIKA Telecommunication, Computing, Electronics and Control
Vol. 24, No. 5, October 2026, pp. 1710∼1720
ISSN: 1693-6930, DOI: 10.12928/TELKOMNIKA.v24i5.27914

Edge-aware adaptive partial differential equation image inpainting for high-quality restoration

Fouzia Hamadache[1,2], Zine-Eddine Baarir[2,3], Nacira Diffellah[1,4], Abdelmalik Ahmed-Taleb[5], Tewfik Bekkouche[6], Rabah Hamdini[1,4]

[1]Institute of Electronics and Telecommunications (IET), University of Mohamed El Bachir El Ibrahimi, Bordj Bou Arreridj, Algeria
[2]Departement of Electronic and Automatic Engineering, Mohamed Khider University of Biskra, Biskra, Algeria
[3]VSC Laboratory of Research, Mohamed Khider University of Biskra, Biskra, Algeria
[4]LMSE laboratory of Research, University of Mohamed El Bachir El Ibrahimi, Bordj Bou Arreridj, Algeria
[5]IEMN UMR CNRS 8520, Valenciennes, France
[6]LEPCI Laboratory, Department of Automatic and Intelligent Systems, Faculty of Technology, University of Ferhat Abbas, Setif, Algeria

Article Info

Article history:

Received Mar 2, 2026
Revised Jun 2, 2026
Accepted Jun 30, 2026

Keywords:

Anisotropic diffusion
Bertalmio model
Edge-aware diffusion
Image inpainting
Isophote propagation
PDE-based restoration
Structural preservation

ABSTRACT

Image inpainting aims to reconstruct missing or damaged regions in digital images while preserving structural consistency and visual coherence. Among partial differential equation (PDE)-based approaches, the model introduced by Marcelo Bertalmio is a foundational technique for isophote-driven structure propagation. However, its performance often degrades in large damaged regions. This limitation is mainly caused by insufficient transport strength and isotropic diffusion, which lead to structural blurring. In this paper, we propose an edge-aware adaptive PDE inpainting model that introduces a transport amplification factor and a spatially-adaptive diffusion term to improve edge propagation and structural preservation. Experimental results on various test images demonstrate that the proposed approach improves structural reconstruction. Quantitative evaluation using peak signal-to-noise ratio (PSNR) and structural similarity index (SSIM) metrics confirms higher restoration accuracy and better edge preservation compared with baseline methods.

Corresponding Author:

Fouzia Hamadache
Institute of Electronics and Telecommunications (IET), University of Mohamed El Bachir El Ibrahimi
Bordj Bou Arreridj, Algeria
Email: fouzia.hamadache@univ-bba.dz

1. INTRODUCTION

Image inpainting is a fundamental problem in image processing and computer vision that aims to reconstruct missing or damaged image regions in a visually plausible manner [1], [2]. Its applications include object removal, cultural heritage restoration, old photograph recovery, film post-production, and error concealment in image transmission. The main challenge is to ensure structural coherence and texture consistency while preserving overall visual realism [3]-[5]. Early inpainting approaches were predominantly based on partial differential equations (PDEs), where missing information is reconstructed by propagating geometric structures from the boundary of the damaged region toward its interior [6]-[8]. Among these methods, the seminal work of Bertalmio *et al.* [7] introduced a third-order isophote-driven transport equation inspired by fluid dynamics [9], [10]. Owing to its solid mathematical foundation and geometric interpretation, this model has become a cornerstone of PDE-based inpainting, particularly effective for small missing regions and thin structures. Despite their strong theoretical foundation, classical PDE-based inpainting models still struggle to maintain structural continuity in large missing regions due to weak isophote transport and excessive diffusion. When applied to large damaged areas, the classical formulation suffers from insufficient transport strength, leading to attenuated structure continuation and blurred edges. Moreover, the diffusion component introduces excessive smoothing, reducing the preservation of fine details. These limitations motivate the development of enhanced PDE-based formulations capable of reinforcing structural propagation while maintaining numerical stability and edge preservation. In this work, we propose an improved PDE-based inpainting framework derived from the classical Bertalmio model. Unlike previous incremental extensions, our method introduces a novel transport amplification factor and a spatially-adaptive diffusion term. The scientific contribution lies in the adaptive control of transport strength and diffusion according to local edge information, which is not present in previous models. The proposed approach incorporates an adaptive transport amplification factor to reinforce isophote propagation and an edge-aware diffusion adjustment to better preserve fine details. A stabilized discretization scheme combining Gaussian pre-smoothing, gradient normalization, intensity projection, and a convergence-based stopping criterion is adopted to ensure robust and stable iterative behavior. Experimental results on benchmark images demonstrate improved structural coherence and quantitative performance compared to representative classical and variational inpainting approaches.

2. RELATED WORK

Image inpainting has been extensively studied over the past two decades, leading to a wide range of reconstruction techniques. Existing approaches are broadly classified into three main categories: diffusion-based, exemplar-based, and hybrid methods.

2.1. Diffusion-based inpainting

Diffusion-based methods reconstruct missing regions by propagating information from known areas through PDEs. The pioneering work of Bertalmio *et al.* [7] introduced a third-order PDE framework that propagates isophotes (lines of equal intensity) into damaged regions. This model preserves geometric structures and edge continuity and has become a cornerstone of PDE-based inpainting. Subsequent extensions incorporated anisotropic diffusion [11], curvature-driven diffusion [12], and higher-order regularization terms to improve smoothness and structural fidelity. These models are particularly effective for small missing regions and thin geometric structures. However, their performance degrades in large damaged areas, where insufficient transport strength and excessive diffusion often lead to blurred edges and loss of fine details. Several adaptive strategies have been proposed to mitigate these limitations, including spatially varying diffusion coefficients and edge-guided transport mechanisms. Nevertheless, achieving a balance between strong structure propagation and numerical stability remains a challenging problem [8], [12]-[14].

2.2. Exemplar-based inpainting

Exemplar-based approaches reconstruct missing regions by copying similar patches from known parts of the image. The influential method of Criminisi *et al.* [15] introduced a priority-driven patch filling strategy based on confidence and data terms, enabling improved structure continuation. A major advancement in this category is the PatchMatch algorithm [16], which provides a fast randomized method for approximate nearest-neighbor patch search. PatchMatch has enabled efficient large-scale image editing and has been integrated into various practical inpainting systems. Exemplar-based methods generally achieve superior performance in texture-rich regions and large missing areas. However, they may suffer from structural inconsistencies when long-range geometric continuation is required [8], [17], [18].

2.3. Hybrid and learning-based methods

Hybrid methods attempt to combine the strengths of diffusion-based and exemplar-based approaches. Typically, geometric structures are first reconstructed using PDE-based techniques, followed by texture synthesis through patch-based strategies [19]. Such combinations aim to improve both structural coherence and texture realism [20]. More recently, deep learning approaches have emerged, employing convolutional neural networks and generative models for data-driven inpainting [21], [22]. Although these models produce visually impressive results, they generally require large training datasets and substantial computational resources. Moreover, in restoration-oriented applications, the hallucination of non-authentic content may be undesirable.

It is important to emphasize that the objective of the proposed method differs from that of data-driven generative inpainting approaches [21]. While deep learning models can synthesize visually plausible textures and complete large missing regions, the reconstructed content may not strictly correspond to the original image structures, as it is partially inferred from learned priors [5]. In controlled restoration scenarios, such as scientific imaging, cultural heritage preservation, or medical image reconstruction, structural fidelity and deterministic behavior are often preferred over generative realism. In such contexts, the introduction of hallucinated structures may lead to misleading interpretations [23]. The proposed PDE-based framework preserves mathematical interpretability, does not rely on external training data, and reconstructs missing regions by propagating existing geometric information from the image itself. Therefore, the present study focuses on deterministic, structure-driven restoration rather than data-driven generative inpainting.

2.4. Motivation and positioning of the proposed method

Despite substantial progress, diffusion-based methods remain attractive due to their mathematical interpretability, low computational complexity, and suitability for structure-preserving restoration [7]-[8]. However, classical PDE models, including the Bertalmio formulation, still face challenges in balancing transport strength, detail preservation, and numerical stability [9], [10]. Motivated by these observations, our work focuses on enhancing the original PDE framework through adaptive transport amplification and edge-aware diffusion adjustment. Unlike exemplar-based or learning-based approaches, the proposed method preserves the deterministic and structure-oriented nature of PDE inpainting while improving robustness and structural coherence. This makes it particularly suitable for controlled restoration scenarios where interpretability and stability are essential.

2.5. Comparative methods

To evaluate the effectiveness of the proposed PDE-based inpainting framework, we compare it against the following benchmark methods:

- Distorted image reconstruction method with trimmed median [24]: this method employs a spatial filtering technique to restore corrupted pixels. By computing the trimmed median of the local neighborhood, it aims to remove noise and fill missing gaps while preserving local structures. However, it often struggles with larger missing regions, which can result in noticeable structural blurring.
- Adaptive Euler's elastica inpainting with discrete gradient optimization [25]: this variational approach reconstructs missing structures by minimizing curvature-based energy functionals with adaptive parameter estimation, providing strong geometric continuity, especially in large missing regions.

These comparative methods allow us to assess the improvements offered by the proposed adaptive transport and edge-aware diffusion mechanisms in terms of structural coherence and quantitative metrics such as peak signal-to-noise ratio (PSNR) and structural similarity index (SSIM).

3. PROPOSED METHOD

3.1. PDE formulation

The classical inpainting model introduced by Bertalmio *et al.* [7] propagates isophotes within the missing region using a third-order PDE. The evolution of the image intensity $I(x, y, t)$ is given by:

$$\frac{\partial I}{\partial t} = \nabla^{\perp} I \cdot \nabla(\Delta I) \tag{1}$$

where $\nabla^{\perp} I = (-I_y, I_x)$ denotes the direction orthogonal to the image gradient (isophote direction), and ΔI is the Laplacian operator, ensuring curvature-driven propagation. To improve numerical stability and reduce noise amplification, an anisotropic diffusion term can be added:

$$\frac{\partial I}{\partial t} = \nabla^{\perp} I \cdot \nabla(\Delta I) + \nabla \cdot (c \nabla I) \tag{2}$$

where the diffusion coefficient c is defined as:

$$c = \frac{1}{1 + \frac{|\nabla I|^2}{K}} \tag{3}$$

with K controlling edge preservation.

3.2. Adaptive transport factor

While effective for small regions, the classical PDE may lack sufficient transport strength in large missing areas. Novelty of the proposed approach: unlike previous adaptive PDE methods that adjust only the diffusion coefficient, our approach introduces two complementary and original mechanisms:
- A transport amplification factor α that directly strengthens isophote propagation in large missing regions
- A spatially-adaptive diffusion term that preserves edges by reducing excessive smoothing

The proposed model is formulated as:

$$\frac{\partial I}{\partial t} = \alpha \nabla^{\perp} I \cdot \nabla(\Delta I) + \nabla \cdot (c\nabla I) \tag{4}$$

where $\alpha > 1$ strengthens isophote propagation, and $\alpha = 1$ reduces to the classical model. The diffusion parameter can also be adapted to enhance fine detail preservation:

$$K_{\text{adapt}} = \beta K, \tag{5}$$

where $\beta < 1$ increases sensitivity to edges.

3.3. Parameter selection and justification

The parameters α and β were empirically selected based on preliminary experiments to balance edge propagation and diffusion stability. A systematic three-step procedure was adopted:

Step 1 – grid search
- α tested: $\{1.0, 1.01, 1.02, 1.03, ..., 1.1\}$
- K tested: $\{0.001, 0.002, 0.003, 0.004, ...0.009\}$
- σ tested: $\{0.5, 1.0, 1.5\}$

Step 2 – selection criteria
- Maximization of PSNR and SSIM on validation images
- Numerical stability (convergence within 500 iterations)
- Absence of visual artifacts

Step 3 – retained values
- $\alpha = 1.08$: best trade-off between structural propagation and stability
- $K = 0.004$: optimal edge preservation
- $\sigma = 1.0$: sufficient smoothing without loss of fine details
- $\Delta t_t = 0.0008$, $\Delta t_d = 0.15$: ensuring numerical stability

Sensitivity analysis
- $\alpha \in [1.0, 1.1]$: stable performance.
- $\alpha > 1.1$: numerical instabilities appear
- $K \in [0.003, 0.005]$: visually disimilar results
- $K < 0.001$: residual noise; $K > 0.009$: excessive smoothing

All parameters were kept constant across all experiments to ensure reproducibility.

3.4. Numerical discretization and stabilization

The PDE is discretized using finite differences in space and explicit time marching:

$$I^{k+1} = I^k + \Delta t_t\, \alpha\, T(I^k) + \Delta t_d\, D(I^k) \tag{6}$$

where $T(I)$ denotes the transport term and $D(I)$ the anisotropic diffusion term. To ensure stability and robustness, we adopt Gaussian pre-smoothing defined as $I_s = G_\sigma * I$, gradient normalization computed as $|\nabla I| = \sqrt{I_x^2 + I_y^2 + \varepsilon}$ to avoid numerical instability, intensity projection to maintain pixel values within the valid range $I \leftarrow \min(\max(I, 0), 1)$, and a convergence criterion based on the relative ℓ_2-norm given by $\frac{\|I^{k+1} - I^k\|_2}{\|I^k\|_2} < 10^{-6}$. The computational complexity is $\mathcal{O}(MNK_{\max})$, where $M \times N$ denotes the image size and $K_{\max}$ the maximum number of iterations. To provide a clearer understanding of the interaction between the transport and adaptive diffusion mechanisms, the operational workflow of the proposed algorithm is illustrated in Figure 1.

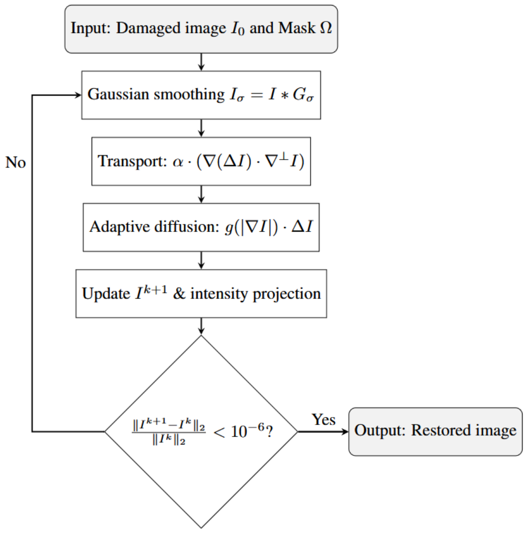

Figure 1. Flowchart of the proposed edge-aware adaptive PDE inpainting algorithm

3.5. Algorithm

The proposed method is summarized in Algorithm 1. It iteratively propagates isophotes within the missing regions while applying edge-aware diffusion, Gaussian smoothing, gradient normalization, and intensity projection to maintain numerical stability.

Algorithm 1 Improved bertalmio PDE-based inpainting

Require: Original image $I_0 \in \mathbb{R}^{M\times N}$, binary mask Ω, maximum iterations $K_{\max}$, transport step Δt_t, diffusion step Δt_d, diffusion parameter K, Gaussian smoothing σ, transport factor α
Ensure: Inpainted image I

```
Initialize I ← I_0
for k = 1 to K_max do
    I^prev ← I
  1) Isophote transport
    I_s ← G_σ * I                                   ▷ Gaussian smoothing
    (I_x, I_y) ← ∇I_s
    |∇I_s| ← sqrt(I_x^2 + I_y^2 + ϵ)
    N_x ← I_x/|∇I_s|, N_y ← I_y/|∇I_s|
    ΔI ← ∇^2 I, (ΔI_x, ΔI_y) ← ∇(ΔI)
    β ← (−N_y)ΔI_x + N_x ΔI_y
    I(Ω) ← I(Ω) + Δt_t · α · β(Ω)
  2) Anisotropic diffusion
    (I_x, I_y) ← ∇I
    c ← 1/(1 + (I_x^2 + I_y^2)/K)
    div ← ∇ · (c∇I)
    I(Ω) ← I(Ω) + Δt_d · div(Ω)
    I ← min(max(I, 0), 1)
    if ||I − I^prev||_2 / ||I^prev||_2 < 10^−6 then
        break
    end if
end for
return I
```

4. RESULTS AND DISCUSSION

To evaluate the effectiveness of the proposed adaptive PDE-based inpainting method, we conducted experiments on a diverse set of images from the Berkeley segmentation dataset (BSDS500) [26], which provides a variety of natural scenes with different structural and textural complexities. Two types of degradation masks are considered to evaluate the inpainting performance. Mask1 consists of irregular yet structured curved missing regions, forming connected stroke-like patterns across the image. This mask is designed to assess the ability of the method to restore fine structures and maintain local continuity. Mask2, in contrast, represents a structured degradation composed of larger contiguous missing areas, including text-shaped regions (watermark-like patterns). This mask evaluates the capability of the method to reconstruct extended regions and ensure coherent long-range structural propagation.

The inpainted results were quantitatively assessed using PSNR [27]-[29] and SSIM [29]-[31], which measure pixel-wise fidelity and perceptual structural similarity, respectively. PSNR reflects reconstruction accuracy, while SSIM emphasizes the preservation of structural features and overall perceptual quality. The PSNR is computed as:

$$\text{PSNR} = 10\log_{10}\left(\frac{MAX_I^2}{\text{MSE}}\right) \tag{7}$$

where MAX_I is the maximum possible pixel value and MSE is the mean squared error between the original image I and the inpainted image $\hat{I}$:

$$\text{MSE} = \frac{1}{MN}\sum_{i=1}^{M}\sum_{j=1}^{N}\left(I(i,j) - \hat{I}(i,j)\right)^2 \tag{8}$$

The SSIM is computed as:

$$\text{SSIM}(I,\hat{I}) = \frac{(2\mu_I\mu_{\hat{I}} + C_1)(2\sigma_{I\hat{I}} + C_2)}{(\mu_I^2 + \mu_{\hat{I}}^2 + C_1)(\sigma_I^2 + \sigma_{\hat{I}}^2 + C_2)} \tag{9}$$

where I is the original image, $\hat{I}$ is the inpainted image, μ and σ denote local mean and variance, $\sigma_{I\hat{I}}$ is the local covariance, and C_1, C_2 are small constants. Figure 2 shows the test images selected for the experimental evaluation. Figures 2(a) to (h) present the eight reference images used in our experiments. Two masking patterns were applied, as illustrated in Figure 3. Figure 3(a) (Mask1) consists of irregular curved missing regions, while Figure 3(b) (Mask2) represents larger contiguous missing areas.

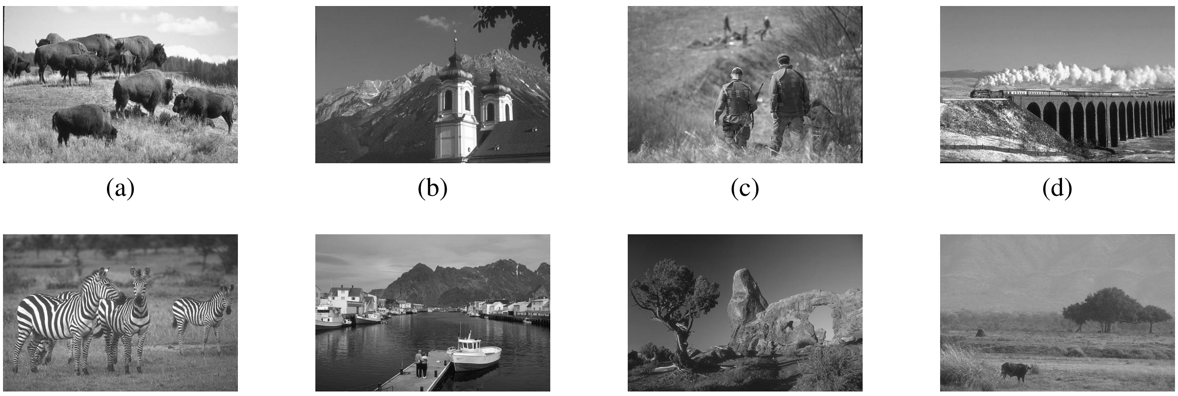

(a) (b) (c) (d)

(e) (f) (g) (h)

Figure 2. Reference test images: (a) 38092, (b) 126007, (c) 170057, (d) 182053, (e) 219090, (f) 253027, (g) 295087, and (h) 296007

(a) (b)

Figure 3. Masks used for image inpainting experiments: (a) Mask1 and (b) Mask2

4.1. Quantitative evaluation

Table 1 presents the quantitative comparison between the trimmed median method [24], the adaptive Euler elastica approach [25], and the proposed method under both masking scenarios. Table 1, shows that the proposed method consistently achieves the highest PSNR and SSIM values across all test images and masking configurations. For Mask1, it preserves fine details and structural continuity. For Mask2, the adaptive transport amplification improves isophote propagation, leading to better geometric reconstruction compared to the baseline methods.

The average results further confirm the superiority of the proposed approach. Under Mask1, it attains the highest mean PSNR (30.1343 dB) and SSIM (0.93657), outperforming both the trimmed median and adaptive Euler elastica methods. The same trend is observed for Mask2, where the proposed method achieves the best mean PSNR (30.8245 dB) and SSIM (0.94684). Overall, the consistent improvement in quantitative metrics demonstrates the robustness and enhanced reconstruction capability of the proposed inpainting framework.

Table 1. Quantitative comparison of PSNR (dB) and SSIM values for image inpainting using trimmed median, adaptive Euler elastica, and the proposed method under Mask1 and Mask2

Image.jpg	Mask	Trimmed median		Adaptive Euler elastica		Proposed	
		PSNR (dB)	SSIM	PSNR (dB)	SSIM	PSNR (dB)	SSIM
38092	Mask1	27.7560	0.91871	27.8948	0.87860	29.4995	0.92764
	Mask2	27.1893	0.92610	27.3959	0.88326	29.1254	0.93389
126007	Mask1	27.9483	0.93879	29.6092	0.92130	29.9560	0.94501
	Mask2	29.9318	0.95066	30.8467	0.93069	31.7043	0.95654
170057	Mask1	31.0474	0.92774	31.6092	0.92947	32.3449	0.94236
	Mask2	31.9959	0.93604	32.7071	0.93969	33.4784	0.95311
182053	Mask1	26.0871	0.92384	25.4707	0.89990	27.0330	0.93153
	Mask2	27.2204	0.94050	26.2018	0.91670	28.2300	0.94900
219090	Mask1	28.5245	0.93253	28.1673	0.89501	29.9536	0.93889
	Mask2	27.9201	0.93285	28.0051	0.89735	29.2746	0.94200
253027	Mask1	24.1626	0.90953	23.8170	0.88230	25.1050	0.91832
	Mask2	23.0839	0.91238	23.4064	0.89180	24.3400	0.92700
295087	Mask1	30.1797	0.93094	28.6956	0.88094	30.7250	0.93349
	Mask2	31.2906	0.94311	29.2801	0.89043	32.0997	0.94574
296007	Mask1	35.4982	0.95112	34.1768	0.91889	36.4572	0.95532
	Mask2	37.1673	0.96310	35.2960	0.92868	38.3438	0.96681
Mean	Mask1	28.9005	0.92912	28.6801	0.90084	30.1343	0.93657
	Mask2	29.4749	0.93810	29.1424	0.90991	30.8245	0.94684

4.2. Sensitivity analysis

To further validate the robustness of the proposed adaptive formulation, a sensitivity analysis was conducted with respect to the main adaptive parameters: the transport amplification factor α and the diffusion scaling parameter β.

4.2.1. Influence of the transport amplification factor

The transport amplification factor α controls the strength of isophote propagation, with $\alpha = 1$ corresponding to the classical Bertalmio formulation. Experimental evaluation shows that increasing α enhances reconstruction quality up to an optimal range, beyond which minor oscillatory effects may slightly reduce performance. These results confirm that the adaptive transport mechanism effectively strengthens structural continuation while maintaining numerical stability when appropriately bounded.

4.2.2. Influence of the diffusion scaling parameter

The diffusion scaling parameter β regulates edge preservation through the adapted diffusion coefficient. Experiments show that moderate reduction of diffusion strength enhances edge sharpness and structural consistency. Excessive reduction may introduce slight texture discontinuities, whereas larger diffusion values produce smoother but slightly blurred reconstructions. The results confirm that the best trade-off between smoothing and edge preservation is obtained for intermediate β values.

4.2.3. Convergence behavior

The convergence criterion $\frac{\|I^{k+1}-I^k\|_2}{\|I^k\|_2} < 10^{-6}$ was satisfied in all experiments within fewer than 300 iterations. No instability was observed within the tested parameter ranges, confirming the numerical robustness of the adaptive transport–diffusion coupling.

4.3. Qualitative evaluation

For qualitative evaluation, three test images (IDs: 38092, 170057, 295087) were analyzed under the Mask1 and Mask2 configurations. Figures 4 and 5 present representative visual reconstruction results obtained with the proposed method, in comparison to the trimmed median and adaptive Euler elastica approaches. In each figure, images from left to right correspond to the corrupted input, the trimmed median inpainting, the adaptive Euler elastica method, and the proposed method.

Figure 4. Inpainting results for test images 38092, 170057, and 295087. Left to right: corrupted image with Mask 1, restored by trimmed median, adaptive Euler elastica, and proposed method

Figure 5. Inpainting results for test images 38092, 170057, and 295087. Left to right: corrupted image with Mask 2, restored by trimmed median, adaptive Euler elastica, and proposed method

Qualitative analysis shows that the proposed method achieves smoother region filling, better edge continuity, and improved preservation of fine textures and structural details. By contrast, the trimmed median method often introduces noticeable blurring, particularly in regions with fine structures, while the adaptive Euler elastica approach may generate minor artifacts in textured areas. Overall, the proposed framework produces more coherent and visually natural reconstructions, with edges and textures consistently maintained across both Mask1 and Mask2 scenarios. These qualitative observations align well with the quantitative improvements reported in Table 1, confirming the effectiveness of the proposed approach in preserving structural and textural fidelity under different masking conditions.

5. CONCLUSION

In this study, we presented an enhanced edge-aware adaptive PDE-based model for image inpainting. By refining the balance between transport and diffusion processes through adaptive parameters, our approach effectively overcomes the blurring artifacts commonly associated with traditional Bertalmio-type models. Experimental results show consistent improvements in PSNR and SSIM, demonstrating enhanced structural reconstruction and edge preservation compared with the benchmark methods. These quantitative findings are supported by qualitative visual analysis, which confirms that the proposed method achieves smoother region filling, better edge continuity, and improved preservation of fine textures and structural details.

Despite these promising results, the proposed method has some limitations. The method is currently limited to grayscale images, and the number of test images remains relatively restricted. Future work will explore hybrid approaches that integrate the proposed adaptive PDE framework with deep learning models to address complex textures and large semantic gaps in high-resolution images. Extending the framework to color images, increasing the dataset size for more comprehensive validation, and comparing with exemplar-based methods, PatchMatch, and deep learning-based inpainting are also among our research directions.

ACKNOWLEDGMENTS

The authors would like to thank their home institutions for support.

FUNDING INFORMATION

Authors state no funding involved.

AUTHOR CONTRIBUTIONS STATEMENT

This journal uses the Contributor Roles Taxonomy (CRediT) to recognize individual author contributions, reduce authorship disputes, and facilitate collaboration.

Name of Author	C	M	So	Va	Fo	I	R	D	O	E	Vi	Su	P	Fu
Fouzia Hamadache	✓	✓	✓	✓	✓			✓	✓	✓	✓	✓		
Zine-Eddine Baarir	✓	✓	✓	✓	✓				✓	✓	✓	✓		
Nacira Diffellah	✓	✓	✓	✓	✓			✓	✓	✓	✓	✓		
Abdelmalik Ahmed-Taleb	✓	✓	✓	✓	✓				✓	✓	✓	✓		
Tewfik Bekkouche	✓	✓	✓	✓	✓			✓	✓	✓	✓			
Rabah Hamdini	✓	✓	✓	✓	✓				✓	✓	✓			

C	: **C**onceptualization	I	: **I**nvestigation	Vi	: **Vi**sualization
M	: **M**ethodology	R	: **R**esources	Su	: **Su**pervision
So	: **So**ftware	D	: **D**ata Curation	P	: **P**roject Administration
Va	: **Va**lidation	O	: Writing - **O**riginal Draft	Fu	: **Fu**nding Acquisition
Fo	: **Fo**rmal Analysis	E	: Writing - Review & **E**diting		

CONFLICT OF INTEREST STATEMENT

Authors state no conflict of interest.

DATA AVAILABILITY

The data supporting the findings of this study are openly available from the Berkeley Segmentation Dataset and Benchmark (BSDS300), originally introduced by Martin *et al.* (2001) [26]. The dataset used in this study can be accessed publicly through the official Berkeley Segmentation Dataset and Benchmark website at https://www2.eecs.berkeley.edu/Research/Projects/CS/vision/bsds/BSDS300/html/dataset/images.html.

REFERENCES

[1] O. Elharrouss, N. Almaadeed, S. Al-Maadeed, and Y. Akbari, "Image Inpainting: A Review," *Neural Processing Letters*, vol. 51, no. 2, pp. 2007–2028, 2020, doi: 10.1007/s11063-019-10163-0.

[2] H. Li, L. Hu, J. Liu, J. Zhang, and T. Ma, "A review of advances in image inpainting research," *Imaging Science Journal*, vol. 72, no. 5, pp. 669–691, 2024, doi: 10.1080/13682199.2023.2212572.

[3] J. Li, F. He, L. Zhang, B. Du, and D. Tao, "Progressive reconstruction of visual structure for image inpainting," in *Proceedings of the IEEE International Conference on Computer Vision*, 2019, pp. 5961–5970, doi: 10.1109/ICCV.2019.00606.

[4] R. Zhang, W. Quan, Y. Zhang, J. Wang, and D. M. Yan, "W-Net: Structure and Texture Interaction for Image Inpainting," *IEEE Transactions on Multimedia*, vol. 25, pp. 7299–7310, 2023, doi: 10.1109/TMM.2022.3219728.

[5] Q. Wang, S. He, M. Su, and F. Zhao, "Image Inpainting Methods: A Review of Deep Learning Approaches," *Symmetry*, vol. 18, no. 1, p. 94, 2026, doi: 10.3390/sym18010094.

[6] D. C. P. Devshri, "Review of Partial Differential Equations in Image Processing: Edge Detection, Restoration, and Beyond," *International Journal of Research & Technology*, vol. 12, no. 4, pp. 92–99, 2024.

[7] M. Bertalmio, G. Sapiro, V. Caselles, and C. Ballester, "Image Inpainting," in *SIGGRAPH 2000 - Proceedings of the 27th Annual Conference on Computer Graphics and Interactive Techniques*, 2000, pp. 417–424, doi: 10.1145/344779.344972.

[8] A. K. Al-Jaberi and E. M. Hameed, "A Review of PDE Based Local Inpainting Methods," in *Journal of Physics: Conference Series*, 2021, p. 12149, doi: 10.1088/1742-6596/1818/1/012149.

[9] C. Ballester, M. Bertalmío, V. Caselles, L. Garrido, A. Marques, and F. Ranchin, "An inpainting- based deinterlacing method," *IEEE Transactions on Image Processing*, vol. 16, no. 10, pp. 2476–2491, 2007, doi: 10.1109/TIP.2007.903844.

[10] M. Bertalmío, V. Caselles, S. Masnou, and G. Sapiro, "Inpainting," *in Computer Vision: A Reference Guide*, Springer, 2021, pp. 670–687, doi: 10.1007/978-3-030-63416-2_249.

[11] J. Weickert, "ECMI Anisotropic Diffusion in Image Processing," *European Consortium for Mathematics in Industry*, vol. 1, p. 165, 1998.

[12] T. F. Chan and J. Shen, "Nontexture Inpainting by Curvature-Driven Diffusions," *Journal of Visual Communication and Image Representation*, vol. 12, no. 4, pp. 436–449, Dec. 2001, doi: 10.1006/jvci.2001.0487.

[13] H. Li, W. Luo, and J. Huang, "Localization of Diffusion-Based Inpainting in Digital Images," *IEEE Transactions on Information Forensics and Security*, vol. 12, no. 12, pp. 3050–3064, 2017, doi: 10.1109/TIFS.2017.2730822.

[14] R. A. Frick and M. Steinebach, "DiffSeg: Towards Detecting Diffusion-Based Inpainting Attacks Using Multi-Feature Segmentation," in *IEEE Computer Society Conference on Computer Vision and Pattern Recognition Workshops*, 2024, pp. 3802–3808, doi: 10.1109/CVPRW63382.2024.00384.

[15] A. Criminisi, P. Pérez, and K. Toyama, "Region filling and object removal by exemplar-based image inpainting," in *IEEE Transactions on Image Processing*, 2004, pp. 1200–1212, doi: 10.1109/TIP.2004.833105.

[16] C. Barnes, E. Shechtman, A. Finkelstein, and D. B. Goldman, "PatchMatch: A randomized correspondence algorithm for structural image editing," in *ACM Transactions on Graphics, ACM*, 2009, pp. 1–11, doi: 10.1145/1531326.1531330.

[17] S. Lou, Q. Fan, F. Chen, C. Wang, and J. Li, "Preliminary investigation on single remote sensing image inpainting through a modified GAN," in *2018 10th IAPR Workshop on Pattern Recognition in Remote Sensing, PRRS 2018*, 2018, pp. 1–6, doi: 10.1109/PRRS.2018.8486163.

[18] H. Liu, X. Bi, G. Lu, and W. Wang, "Exemplar-Based Image Inpainting with Multi-Resolution Information and the Graph Cut Technique," *IEEE Access*, vol. 7, pp. 101641–101657, 2019, doi: 10.1109/ACCESS.2019.2931064.

[19] W. Casaca, M. Boaventura, M. P. De Almeida, and L. G. Nonato, "Combining anisotropic diffusion, transport equation and texture synthesis for inpainting textured images," *Pattern Recognition Letters*, vol. 36, pp. 36–45, 2014, doi: 10.1016/j.patrec.2013.08.023.

[20] L. Liao, J. Xiao, Z. Wang, C. W. Lin, and S. Satoh, "Image Inpainting Guided by Coherence Priors of Semantics and Textures," in *Proceedings of the IEEE Computer Society Conference on Computer Vision and Pattern Recognition, Los Alamitos, CA, USA: IEEE Computer Society*, Jun. 2021, pp. 6535–6544, doi: 10.1109/CVPR46437.2021.00647.

[21] K. Nazeri, E. Ng, T. Joseph, F. Z. Qureshi, and M. Ebrahimi, "EdgeConnect: Generative Image Inpainting with Adversarial Edge Learning," *arXiv preprint* arXiv:1901.00212, 2019, doi: 10.48550/arXiv.1901.00212.

[22] W. Quan, J. Chen, Y. Liu, D. M. Yan, and P. Wonka, "Deep Learning-Based Image and Video Inpainting: A Survey," *International Journal of Computer Vision*, vol. 132, no. 7, pp. 2367–2400, 2024, doi: 10.1007/s11263-023-01977-6.

[23] Z. Xu *et al.*, "A Review of Image Inpainting Methods Based on Deep Learning," *Applied Sciences* (Switzerland), vol. 13, no. 20, p. 11189, 2023, doi: 10.3390/app132011189.

[24] D. N. H. Thanh, N. Van Son, and V. B. S. Prasath, "Distorted image reconstruction method with trimmed median," in *Proceedings - 2019 3rd International Conference on Recent Advances in Signal Processing, Telecommunications and Computing*, SigTelCom 2019, 2019, pp. 58–62, doi: 10.1109/SIGTELCOM.2019.8696138.

[25] D. N. H. Thanh, V. B. S. Prasath, S. Dvoenko, and L. M. Hieu, "An adaptive image inpainting method based on euler's elastica with adaptive parameters estimation and the discrete gradient method," *Signal Processing*, vol. 178, p. 107797, 2021, doi: 10.1016/j.sigpro.2020.107797.

[26] D. Martin, C. Fowlkes, D. Tal, and J. Malik, "The Berkeley Segmentation Dataset [online]," pp. 416–423, 2001. [Online]. Available: https://www2.eecs.berkeley.edu/Research/Projects/CS/vision/bsds/BSDS300/html/dataset/images.html

[27] A. Vishwakarma, "Denoising and Inpainting of Sonar Images Using Convolutional Sparse Representation," *IEEE Transactions on Instrumentation and Measurement*, vol. 72, pp. 1–9, 2023, doi: 10.1109/TIM.2023.3246527.

[28] S. Xu, W. Xiang, C. Lv, S. Wang, and G. Liu, "Diversified Image Inpainting with Transformers and Denoising Iterative Refinement," *IEEE Access*, vol. 12, pp. 187068–187080, 2024, doi: 10.1109/ACCESS.2024.3514930.

[29] O. Elharrouss, R. Damseh, A. N. Belkacem, E. Badidi, and A. Lakas, "Transformer-based image and video inpainting: current challenges and future directions," *Artificial Intelligence Review*, vol. 58, no. 4, p. 124, 2025, doi: 10.1007/s10462-024-11075-9.

[30] Z. Wang, A. C. Bovik, H. R. Sheikh, and E. P. Simoncelli, "Image quality assessment: From error visibility to structural similarity," *IEEE Transactions on Image Processing*, vol. 13, no. 4, pp. 600–612, 2004, doi: 10.1109/TIP.2003.819861.

[31] Y. Xing *et al.*, "Time-Variant Image Inpainting via Interactive Distribution Transition Estimation," *IEEE Transactions on Image Processing*, vol. 35, pp. 5107–5122, 2026, doi: 10.1109/TIP.2026.3687440.

BIOGRAPHIES OF AUTHORS

Fouzia Hamadache is a researcher and lecturer at the Institute of Electronics and Telecommunications, Mohamed El Bachir El Ibrahimi University of Bordj Bou Arreridj, Algeria. Her research interests include image processing, power electronics, and FPGA design. She has supervised numerous master's students and actively contributes to both teaching and research projects in her fields of expertise. She can be contacted at email: fouzia.hamadache@univ-bba.dz.

Zine-Eddine Baarir is a Professor of Electrical Engineering at the University of Mohamed Khider – Biskra, Algeria, specializing in signal and image processing. He has a Doctorate and an habilitation in Electronics and leads research in image processing and related applications. He has published numerous scientific works and has actively supervised graduate research in his field. He can be contacted at email: zineeddine.baarir@univ-biskra.dz.

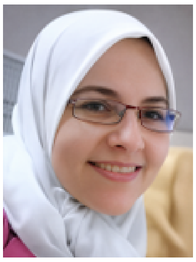

Nacira Diffellah is a researcher and lecturer at the Institute of Electronics and Telecommunications, Mohamed El Bachir El Ibrahimi University of Bordj Bou Arreridj, Algeria. She obtained her engineering degree after working on the analysis and synthesis of digital filters. She then completed a Magister degree focused on the modeling and fuzzy logic control of biotechnological systems, before pursuing a Ph.D. dedicated to image denoising using proximal methods. Her research interests mainly revolve around signal processing and image processing. She can be contacted at email: nacira.diffellah@univ-bba.dz.

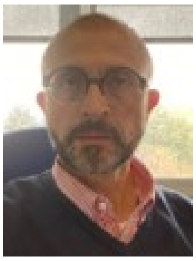

Abdelmalik Ahmed-Taleb received his Ph.D. in Electronics and Microelectronics from Université des Sciences et Technologies de Lille 1 in 1992. He was an associate professor in Calais until 2004, then joined Université Polytechnique des Hauts de France, where he is now a Full Professor and a member of the IEMN DOAE laboratory. His research focuses on computer vision, AI, and machine learning, with interests in segmentation, classification, data fusion, pattern recognition, and applications in biometrics, surveillance, autonomous driving, and medical imaging. He has (co-)authored over 125 papers and (co-)supervised 20 graduate students. His recent work centers on intelligent transportation, road digitization, e-health, and affective computing.He has served as a reviewer for numerous international journals and conferences. He also actively collaborates with industry partners on AI-driven solutions for real-world challenges. He can be contacted at email: abdelmalik.taleb-ahmed@uphf.fr.

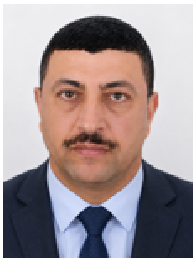

Tewfik Bekkouche received the Engineering and Ph.D. degrees in Electronics in 1990 and 2018, respectively. He is currently a Professor at the University of Setif, Algeria. With a solid academic background and extensive expertise in the field, he is committed to developing secure and innovative solutions in information technology. His research interests include image encryption, biometrics, and information security. He can be contacted at email: tewfik.bekkouche@univ-setif.dz.

Rabah Hamdini is a faculty member at the Institute of Electronics and Telecommunications, University Mohamed El Bachir El Ibrahimi, Bordj BouArréridj, Algeria. He holds a Master's degree in Industrial Computing and a Ph.D. in Automation. His research focuses on signal processing and image processing, particularly on artificial vision techniques for object recognition and image denoising. His interests also include embedded systems, the internet of things (IoT), and intelligent engineering applications. He can be contacted at email: rabah.hamdini@univ-bba.dz.